Vol. 67: 1–14, 2016
doi: 10.3354/cr01347

CLIMATE RESEARCH
Clim Res

Published online January 12

Climate variability and change on the Mongolian Plateau: historical variation and future predictions

Liguang Jiang[1,2], Zhijun Yao[1,*], He Qing Huang[1]

[1]Institute of Geographic Sciences and Natural Resources Research, Chinese Academy of Sciences, 11A Datun Road, Beijing 100101, China

[2]*Present address:* Department of Environmental Engineering, Technical University of Denmark, 2800 Kgs. Lyngby, Denmark

ABSTRACT: In this study, variations in temperature and precipitation over the Mongolian Plateau are analyzed using Climatic Research Unit monthly observations from 1911 to 2010. In addition, the climatology regime of future climate projections is presented using 16 state-of-the-art global climate models participating in the Coupled Model Intercomparison Project Phase 5 under 2 different representative concentration pathway (RCP) emissions scenarios (RCP4.5 and RCP8.5). In the process, changes in the climate normals of 1961–1990 and 2061–2090 are compared. The following results were obtained: (1) Over the past century, the average annual amount of precipitation was 254 ± 5 mm, 67.8% of which appeared in summer (June to August), and no clear trends were found. Temperature exhibited a clear upward trend at a rate of 0.18°C decade^{-1} ($p < 0.001$), and the increases in minimum temperature, mean temperature and maximum temperature were 1.90, 1.78 and 1.59°C, respectively, showing an asymmetric warming process. The winter minimum temperature showed the largest warming trend, at a rate of 0.36°C decade^{-1} ($p < 0.001$). Spatial heterogeneity was apparent for both precipitation and temperature, although these variables exhibited different patterns. (2) During the coming century, increases in precipitation and temperature can be seen under RCP4.5 and RCP8.5, with pronounced larger amplitude changes under RCP8.5. By 2100, the increases in precipitation are 13.3 and 16.1% for RCP4.5 and RCP8.5, respectively, and the increases in mean temperature are 3.5 and 7.1°C. The spatial patterns are more complicated. These results suggest that the Mongolian Plateau will experience significant climate warming and accompanying increased precipitation. Adaptation strategies are needed to improve the capability to respond and adapt to a warmer environment in the coming century.

KEY WORDS: Climate change · CRU · CMIP5 · Mongolian Plateau · Predictions · Temperature · Precipitation

1. INTRODUCTION

In recent years, an international consensus has been achieved among the scientific community concerning climate variability and change and its effects on the environment (Philandras et al. 2011 and reference therein). The importance of investigating regional climate changes associated with global warming is increasingly being recognized. Moreover, the warming trend is significant over arid and semiarid areas, especially semiarid regions, which have taken up approximately 44% of the global annual mean land surface temperature trend (Huang et al. 2012). Any change in climate may provoke extreme weather events, such as heat waves, drought and extreme rainfall events, some of which have the potential to trigger natural disasters.

The Mongolian Plateau is located in an arid to semiarid area in northeastern Asia, consisting of the whole area of Mongolia and the Inner Mongolia Autonomous Region of China in our study. It lies in the transition zone between the westerlies and the East Asian Monsoon, which makes it climatically sensitive (Tian et al. 2014). In addition, this transition

*Corresponding author: yaozj@igsnrr.ac.cn

zone is very sensitive to climate changes due to its geographic location and geomorphological features (Sato et al. 2007). The economy of the Mongolian Plateau relies heavily on livestock, which requires pastures. However, the pastures are strongly affected by climate conditions (Bolortsetseg & Tuvaansuren 1996). Therefore, climate has a significant effect on economic development and local residents' lives. Given that large changes in climate have occurred and are expected to continue in the future (Ni 2003), understanding climate variability and change is an important issue. Our review found few studies on climate variation in this region (e.g. Sato et al. 2007, Kynicky et al. 2009, Davi et al. 2010). In addition, as far as we know, no published research has specifically examined long-term temporal and spatial variations in temperature and precipitation over the Mongolian Plateau. Therefore, it is essential to perform a systematic study in this region.

The Climate Research Unit (CRU) time series dataset (Harris et al. 2014) provided an alternative data source to *in situ* and remotely sensed data, and helped overcome some of the data issues (e.g. short periods of data coverage, low resolution, inhomogeneity, etc.). These reanalysis data have been widely used in regional climate studies (Sen Roy & Sen Roy 2011, Chou et al. 2012, Ferguson & Villarini 2012, Landman & Beraki 2012, Haslinger et al. 2013) or utilized as validation references (Bastola & Francois 2012, Pavlik et al. 2012, Dong et al. 2013b, Gomez-Navarro et al. 2013, Hao et al. 2013, Wang & Zeng 2013).

The Coupled Model Intercomparison Project Phase 5 (CMIP5) provides a unique opportunity to assess the scientific understanding of historical climate variability and possible future change (Wuebbles et al. 2014). The models participating in CMIP5 contain historical simulations and future predictions under different representative concentration pathways (RCPs). RCP4.5 is a stabilization scenario, where total radiative forcing is stabilized before 2100 by employment of technologies and strategies to reduce greenhouse gas (GHG) emissions. RCP8.5 is characterized by increasing GHG emissions over time, representative of scenarios with high GHG concentration levels (Moss et al. 2010, Meinshausen et al. 2011, Taylor et al. 2012). More information about the RCPs can be found in Moss et al. (2010). Multi-model ensembles are nearly always better than any single model; they can counteract deviations of individual models and thus provide statistically superior estimates by enabling pointwise averaging over the multi-model ensemble of simulations (Phillips & Gleckler 2006, Landman & Beraki 2012 and references therein). In this context, using a multi-model ensemble helps improve predictive capabilities for future climate change and provide reliable evaluation results.

In this study, there are 2 principal questions to be addressed: (1) What were the climate conditions of the Mongolian Plateau over the past hundred years, how did the surface air temperature and precipitation change over this period and did these variables rise along with the global trend or show any special characteristics? (2) How will the climate change in the 21st century, and will temperature and precipitation patterns be very different from those in the past?

2. DATA AND METHODOLOGY

2.1. Observational data

Monthly near-surface temperature and precipitation from the most accurate global database, namely, CRU time series 3.21 (CRU TS3.21), were used to reconstruct the temperature and precipitation patterns from 1911 to 2010 in the study area (given in Fig. 1). The near-surface temperature data include mean temperature, maximum temperature and minimum temperature. CRU TS3.21 is a set of monthly climate grids at a resolution of 0.5° × 0.5° and provides best estimates of month-by-month variations (Immerzeel 2008) over a long time span. The data are publicly available online at www.cru.uea.ac.uk/cru/data/hrg.

2.2. Model simulations

Monthly surface air temperature and precipitation data from 16 different models from 2006 to 2099–2100 are used to analyze future climate projections under the RCP4.5 and RCP8.5 scenarios. The data were downloaded from the BADC node of ESGF (http://badc.nerc.ac.uk/browse/badc/cmip5/data; note that an application for access to the data is required). Although some models performed multiple runs starting from different initial conditions, only the first realization (i.e. r1i1p1) from each model was used for the purposes of this study.

2.3. Methods

Observational temperature and precipitation data were calculated on a grid cell-by-grid cell basis for the annual mean and the 4 seasons: December to

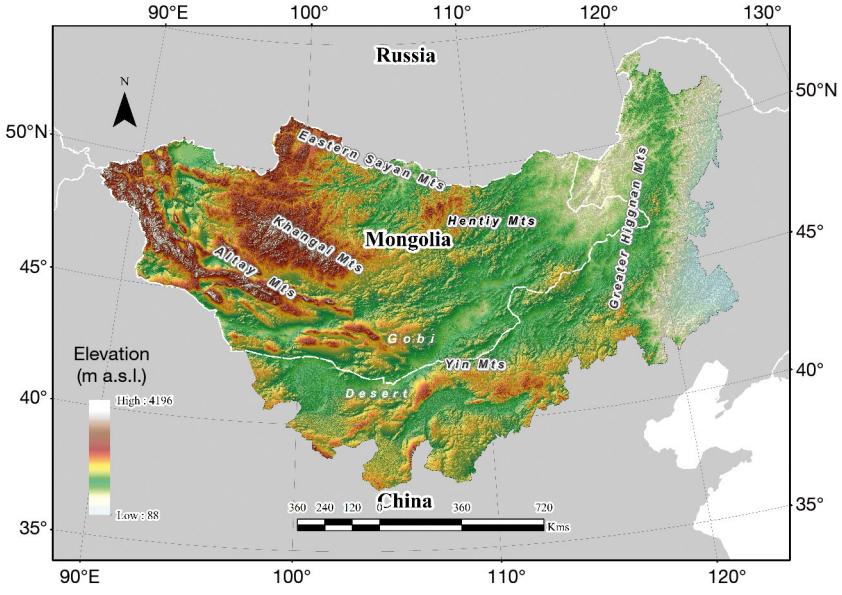

Fig. 1. Location and topography of the study area

February, March to May, June to August and September to November. These gridded data were then averaged (equal weight) across all grid cells in each layer to get regionally averaged data. Trends of temperature and precipitation variation were evaluated according to Yue et al. (2002). A serial correlation and pre-whitening method was applied to remove the effect of correlation on the Mann-Kendall test. The Mann-Kendall test was then applied to the pre-whitened series with the Theil-Sen's slope estimator to obtain the trend and magnitude. A trend is considered significant if it is statistically significant at the 5 % level.

To evaluate the model's performance, simulated historical temperature and precipitation for the period 1961–1990 were compared with CRU data. Several statistical measures such as spatial resemblance, long-term mean climatology, correlation coefficients and standard deviation (SD) were used to assess the relative performance of models. The Taylor diagram has been used to provide a concise statistical summary of the SD, correlation coefficient and root mean square difference (RMSD) in a single diagram (Taylor 2001).

Different CMIP5 model outputs are available at different spatial resolutions, as shown in Table 1. First, these model data were regridded to a 0.5° × 0.5° spatial resolution for consistency via bilinear interpolation, and then all climate data ware bias corrected based on CRU TS3.21 1961–1990 climatology. Temperature data were corrected by using the delta change method (Eq. 1) and precipitation by using relative anomalies and multiplication (Eq. 2) (Terink et al. 2010, Ahlstrom et al. 2012, Berg et al. 2012). The projection data were obtained by averaging across the multi-model ensemble.

Table 1. Climate models used in this study, with institute, resolution and reference period

Model	Institute	Resolution (lon × lat)	Reference period
ACCESS1.3	Australian Commonwealth Scientific and Industrial Research Organization (CSRIO), Australia	192 × 145	1850–2100
BCC-CSM1.1M	Beijing Climate Center (BCC), China	320 × 160	1850–2100
BNU-ESM	Beijing Normal University (BNU), China	128 × 64	1850–2100
CanESM2	Canadian Centre for Climate Modelling and Analysis (CCCma), Canada	128 × 64	1850–2100
CCSM4	National Center for Atmospheric Research (NCAR), USA	288 × 192	1850–2100
CESM1-CAM5	Community Earth System Model Contributors, NSF-DOE-NCAR, USA	288 × 192	1850–2100
CSIRO Mk3.6.0	Commonwealth Scientific and Industrial Research Organization/Queensland Climate Change Centre of Excellence, Australia	192 × 96	1985–2100
CMCC-CM	Centro Euro-Mediterraneo sui Cambiamenti Climatici (CMCC), Italy	480 × 240	1850–2100
CNRM-CM5	Centre National de Recherches Meteorologiques, France	256 × 128	1850–2100
EC-EARTH	European Consortium (EC)	320 × 160	1850–2100
GFDL-ESM2M	Geophysical Fluid Dynamics Laboratory, USA	144 × 90	1861–2100
HadGEM2-ES	Hadley Centre for Climate Prediction and Research/Met Office, UK	192 × 145	1859–2099
IPSL-CM5A-MR	L'Institut Pierre-Simon Laplace, France	144 × 143	1850–2100
MIROC-ESM-CHEM	Center for Climate System Research, National Institute for Environmental Studies, and Frontier Research Center for Global Change, Japan	128 × 64	1850–2100
MPI-ESM-LR	Max Planck Institute for Meteorology, Germany	192 × 96	1850–2100
MRI-CGCM3	Meteorological Research Institute, Japan	320 × 160	1850–2100

$$T_{bc}(y,m) = T_{mod}(y,m) + (\overline{T}_{obs} - \overline{T}_{mod})(m) \quad (1)$$

$$P_{bc}(y,m) = P_{mod}(y,m) \times (\overline{P}_{obs} / \overline{P}_{mod})(m) \quad (2)$$

where T_{bc} and P_{bc} denote the bias-corrected temperature and precipitation time series, respectively; T_{mod} and P_{mod} are the model-simulated time series datasets; $\overline{T}_{obs}$ and $\overline{T}_{mod}$,, $\overline{P}_{obs}$ and $\overline{P}_{mod}$ are the average monthly temperature and average monthly amount of precipitation of the CRU observation and model output, respectively, during the reference period; y is time (month–year); and m denotes location (pixel).

3. RESULTS AND ANALYSIS

In this section, the variability and change in temperature and precipitation of the past century are analyzed, and then, the results from projection under different RCPs are presented. Finally, long-term trends as well as the spatial heterogeneity of climatologies during the 2 periods (1961–1990 and 2061–2090) are compared.

3.1. Validation of CMIP5 models

The Taylor diagram provides a convenient way to compare different models in terms of SD, correlation and centered RMSD (Taylor 2001). The Taylor diagram shows the 3 metrics based on a comparison between CRU observations and each model simulation in turn. The circles centered at the reference point marked CRU and the origin represent the magnitude of RMSD and SD, respectively. The rays denote the correlation. Models with as much variance as the CRU, the least RMSD and the largest correlation are considered the best performers. Each model is represented by a point on the diagram.

Fig. 2 demonstrates the model performance for precipitation and temperature on a monthly basis. It is obvious that all models show a good performance for precipitation, although the magnitude of SD is a little higher, especially in MIROC-SEM-CHEM and CESM1-CAM5. However, the multi-model ensemble is closer to the CRU than any of the individual models. IPSL-CM5A-MR and HadGEM2-ES are superior models regarding the 3 metrics. For temperature, the models all agree concerning the correlation coeffi-

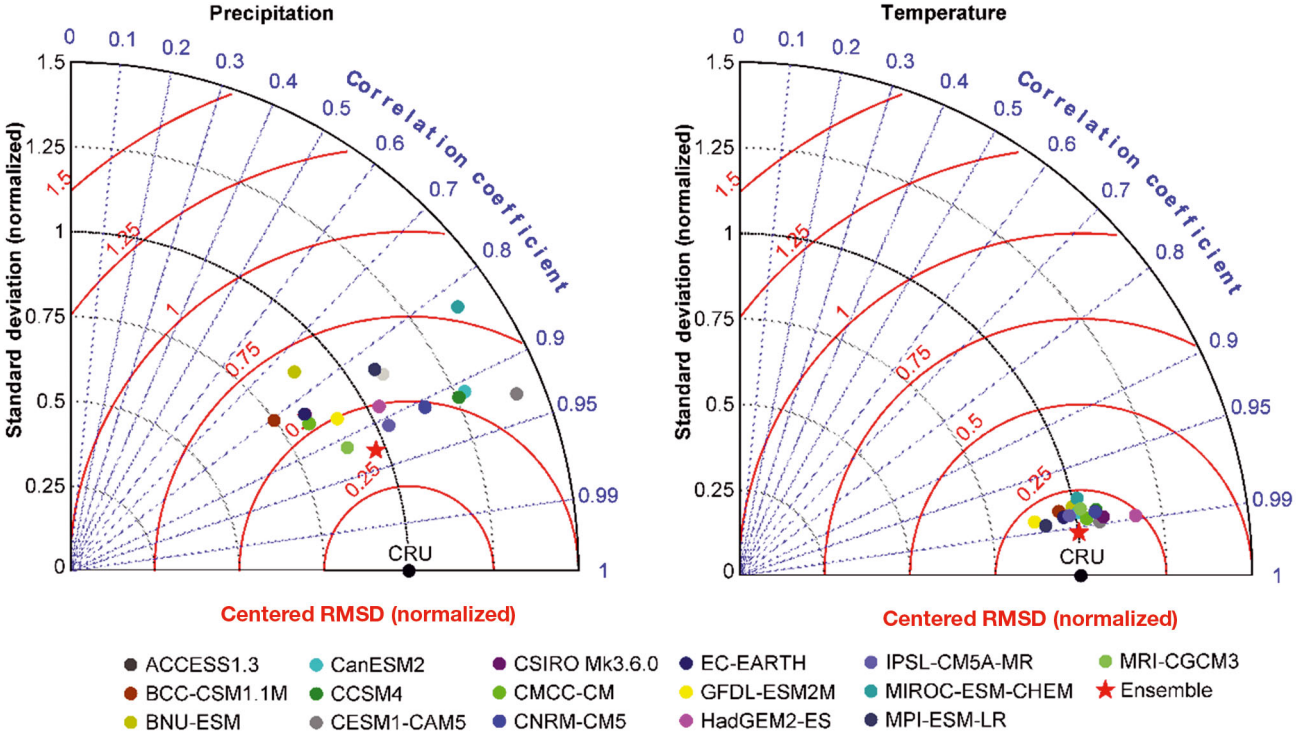

Fig. 2. Taylor diagrams for precipitation and temperature on a monthly scale, comparing Coupled Model Intercomparison Project Phase 5 models and multi-model ensemble simulations with Climatic Research Unit (CRU) observation for the period 1961–1990. RMSD: root mean square difference

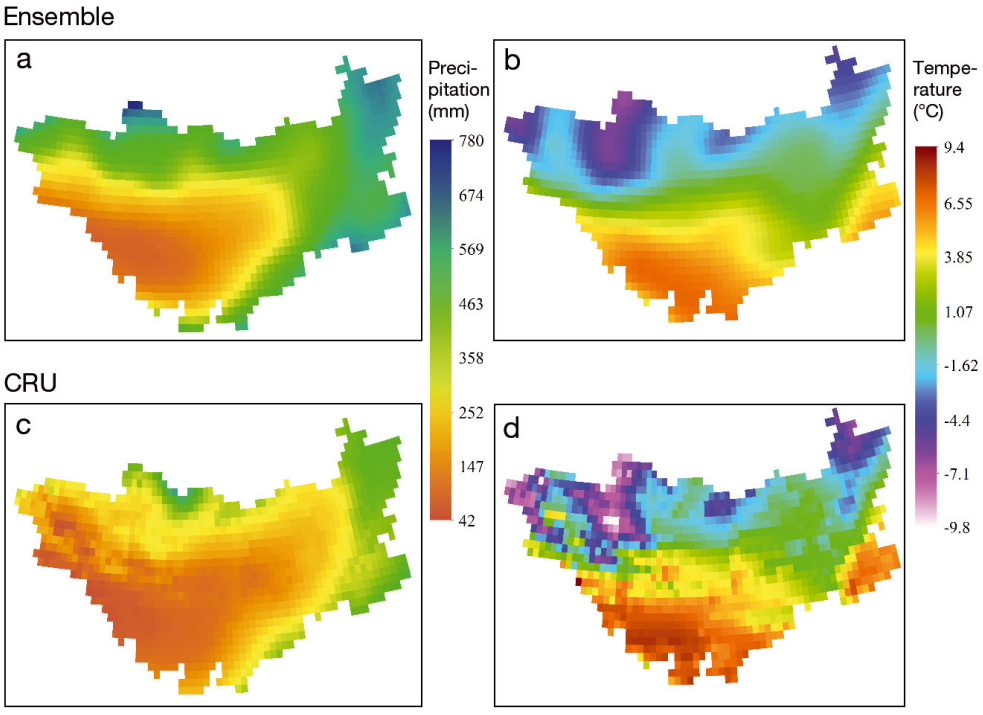

Fig. 3. Annual climatology (1961–1990) of (a) precipitation and (b) temperature from the multi-model ensemble compared to CRU (c) precipitation and (d) temperature

cient and perform markedly better than for precipitation. The multi-model ensemble again shows the best performance.

The spatial patterns of annual climatology are compared between the multi-model ensemble and the CRU over the period 1961–1990. The ensemble simulates the broad patterns of precipitation distribution relatively well but overestimates the intensity, especially in the mountainous areas. The minima and maxima are simulated well in desert areas and the Greater Higgnan Mountains, respectively (Fig. 3a,c). It shows the ability to reproduce precipitation over this region. Meanwhile, the ensemble simulation is comparable with the CRU observation concerning the spatial pattern of temperature, and there is no prominent difference between the patterns. Strictly speaking, the ensemble simulation is too smooth with somewhat lower temperatures in desert areas (Fig. 3b,d).

Results suggest higher confidence for the multi-model ensemble to predict precipitation and temperature reasonably. After a bias-correction procedure, the projections can be used to analyze the possible future scenarios.

3.2. Historical climate variation

We first performed an analysis of temperature and precipitation over the period 1911–2010. Fig. 4 illustrates regionally averaged annual precipitation anomalies and monthly precipitation characteristics. The average annual amount of precipitation was 254 ±

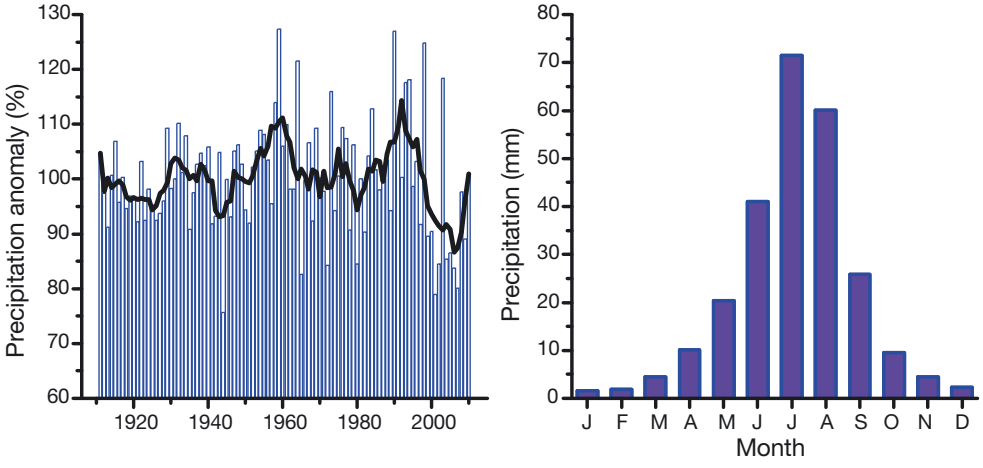

Fig. 4. Regionally averaged annual precipitation anomalies (left) and monthly precipitation (right). Black line: the 5 yr moving average of precipitation anomalies

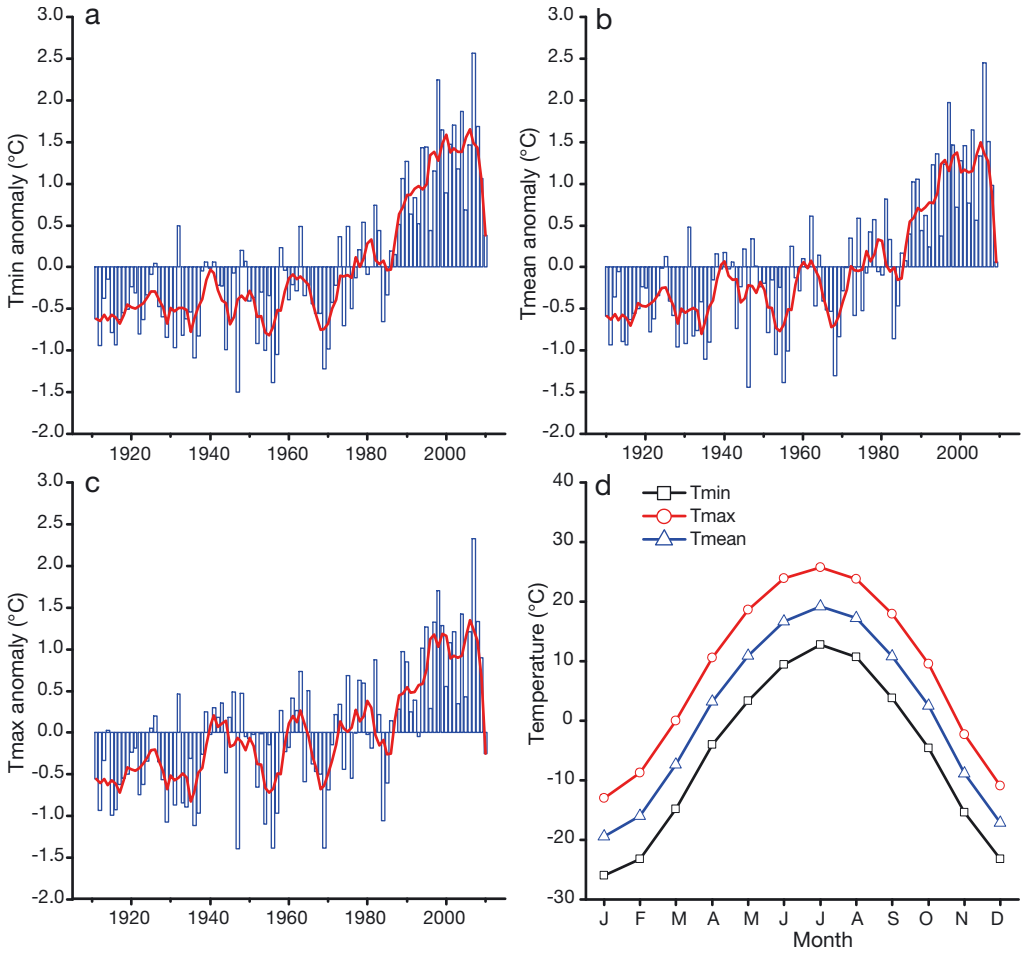

Fig. 5. Regionally averaged annual (a) minimum temperature (Tmin), (b) mean temperature (Tmean) and (c) maximum temperature (Tmax) anomalies (°C), where lines represent the 5 yr moving average of temperature anomalies; (d) average monthly Tmin, Tmax and Tmean

5 mm with a slight negative trend, which is statistically insignificant (95% confidence limit [CL]). Through a 5 yr moving average line (Fig. 4), it can be seen that slightly higher values occurred during the periods 1931–1940, 1952–1963 and 1989–1998. An approximate 10 yr cycle is observed in the annual precipitation pattern. Taking into consideration the monthly precipitation, high precipitation mainly appeared in June to August, accounting for 67.8% of the total annual precipitation. The spring precipitation trend is slightly positive (0.2 mm season^{-1} decade^{-1}), and there is a negative trend in summer (–0.6 mm season^{-1} decade^{-1}), which indicates a decrease in annual precipitation due to the large proportion of total precipitation represented in summer (54.8 to 77.8%). Autumn and winter precipitation does not show a clear trend.

Long time-series temperature data exhibit strong period fluctuations and a clear upward trend (Fig. 5). A warming trend is conspicuous throughout the whole area, with a rate of 0.18°C decade^{-1} ($p < 0.001$). During the period 1911–2010, the increments for minimum temperature, mean temperature and maximum temperature are 1.90, 1.78 and 1.59°C, respectively. It is remarkable that during the most recent 2 decades, temperatures show a statistically significant (99% CL) increase, which is especially pronounced for minimum temperature (Fig. 5a). The average monthly temperatures (Fig. 5d) show large annual fluctuations, which can reach up to 38.7°C. However, the temperature differences vary from month to month. The maximum temperature difference appears in May, while the minimum appears in December. From the perspective of mean temperature, the temperature turns positive in April and then stays above zero until October. The warmest month is July, while the coldest is January.

There are, however, significant seasonal differences. Table 2 shows the seasonal temperature variations. The average warming trend is largest in winter, followed by spring, autumn and summer. The warming rate of winter is twice that of autumn and 4 times that of summer. This suggests that warming is enhanced in the cold season, indicating that temperature variability in the cold season is more sensitive to climate change. Additionally, the minimum tem-

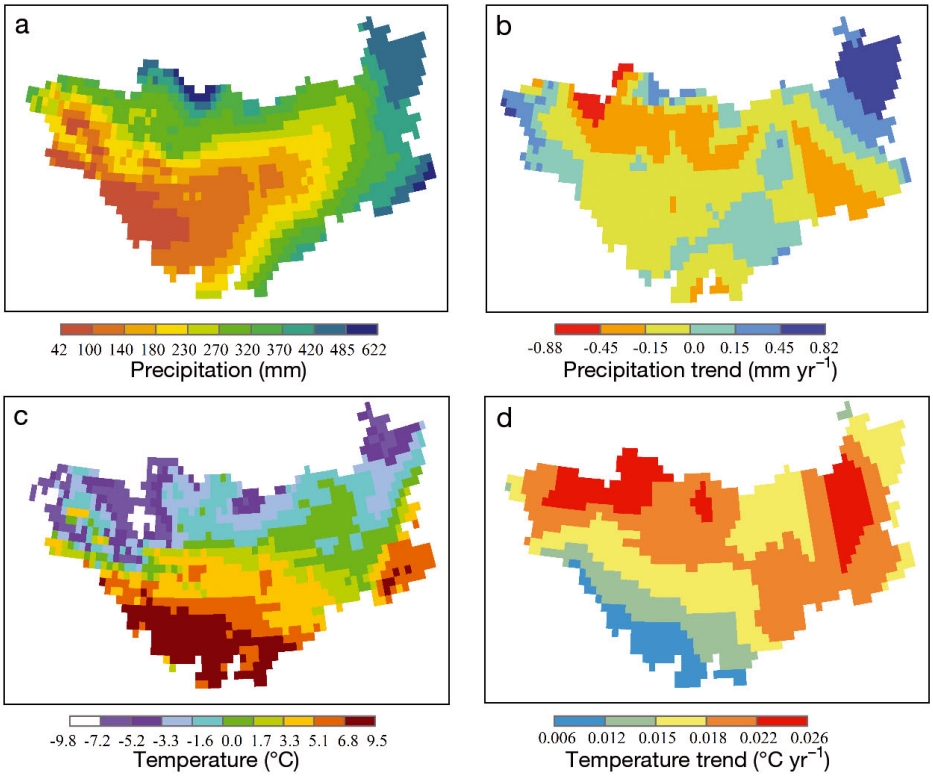

Fig. 6. Spatial pattern of precipitation and temperature and changing trends during 1911–2010. (a) Average annual amount of precipitation; (b) changing trend of precipitation; (c) average annual temperature; (d) changing trend of temperature

perature exhibits higher slopes in all seasons than mean temperature and maximum temperature, revealing that low temperature response is more sensitive to global warming.

The spatial pattern of average annual precipitation over the Mongolian Plateau for the period 1911–2010 is depicted in Fig. 6a. It is obvious that precipitation increases from southwest to northeast. Specifically, high precipitation totals (>300 mm) appear in the north and east, while low precipitation occurs in the desert areas of the centre and south, including the Gobi Desert, the Badain Jaran Desert, the Tengger Desert, the Ulan Buh Desert and the Otindag Sandy Land. Most parts (65.1%) of the Mongolian Plateau experienced a decrease in precipitation. It should be noted that areas with higher precipitation experienced increasing trends, while those with lower precipitation experienced decreasing trends (Fig. 6a,b). In other words, the wet areas got wetter and the dry areas got drier. The areas with higher precipitation (>400 mm) and larger rates of increase (1.5 mm decade^{-1}) were mainly distributed in the Eastern Sayan Mountains and the Greater Higgnan Mountains regions.

Fig. 6c depicts the distribution of average annual temperature. A significant latitudinal gradient can be clearly seen, descending from south to north. The areas with highest temperature are in the desert of Inner Mongolia, with a smaller warming trend (<0.12°C decade^{-1}). In the northern part of the Mongolian Plateau, specifically the Khangai, Altay and northernmost Greater Higgnan mountains, temperatures are below zero. Meanwhile, the spatial pattern of trends is also clearly distinguishable (Fig. 6d). It is worth noting that the areas with the greatest trend in average annual temperature (0.022 to 0.026°C yr^{-1}) are located in mountain regions. One such case is the Khangai Mountains, where precipitation is low and decreasing, showing a warming, drying climate.

Table 2. Linear trends of minimum, mean and maximum temperature series

	Tmin		Tmean		Tmax	
	Slope	Sig.	Slope	Sig.	Slope	Sig.
Spring	0.0235	<0.001	0.0225	<0.001	0.0205	<0.001
Summer	0.0066	0.064	0.0051	0.159	0.0049	0.251
Autumn	0.0156	<0.001	0.0133	0.001	0.0103	0.007
Winter	0.0355	<0.001	0.0325	<0.001	0.0287	<0.001
Year	0.0190	<0.001	0.0178	<0.001	0.0159	<0.001

3.3. Predictions of future climate changes

For predictions of precipitation, the average annual amounts of precipitation are 287 ± 2 and

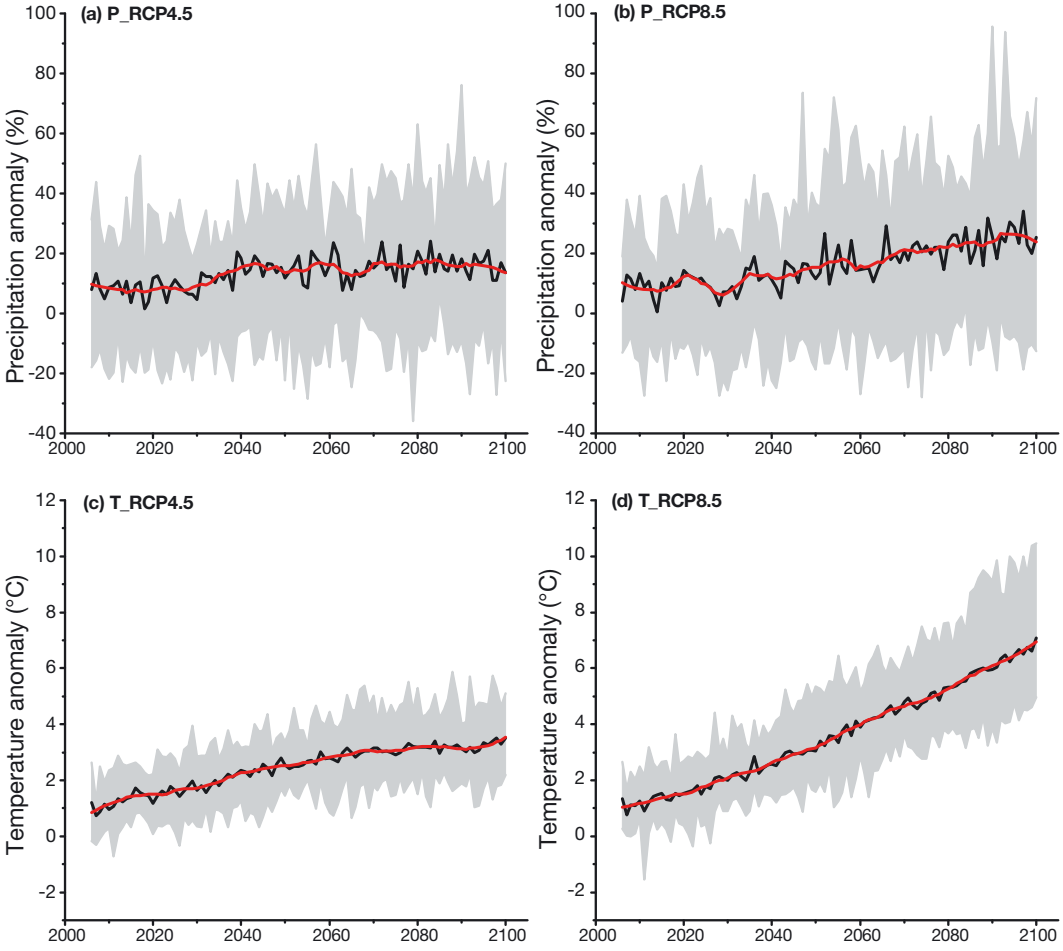

Fig. 7. Regionally averaged (a,b) precipitation (P) and (c,d) temperature (T) anomalies relative to the climate normal (1961–1990) for (a,c) representative concentration pathway (RCP) 4.5 and (b,d) RCP8.5 scenarios based on the 16 Coupled Model Intercomparison Project Phase 5 models. Light gray: individual model simulations; black: multi-model ensemble mean; red: 15 yr moving average

294 ± 3 mm. The Mann-Kendall test indicated that the tendencies for RCP4.5 and RCP8.5 were statistically significant at a 99% CL. Both scenarios show positive trends, with slopes of 2.6 and 5.1 mm decade^{-1}, respectively, although the projected changes show a complex pattern. The precipitation increases are 13.3% (1.5 to 24.0%) and 16.1% (0.6 to 34.1%) for RCP4.5 and RCP8.5, respectively (Fig. 7a,b). The processes are characterized by a high degree of variability, which suggests uneven inter-annual precipitation and extreme precipitation events.

Temperature has risen during the past 3 decades, and the warming trend will continue (Fig. 7c,d). Fig. 7 depicts that the changes in temperature are relatively continuous and smooth. By 2100, it is projected that temperature will have increased by 3.5 and 7.1°C for RCP4.5 and RCP8.5, respectively, relative to the period 1961–1990. The corresponding slopes are 0.26 and 0.64°C decade^{-1} (99% CL). Compared to the changes in precipitation, warming is a relatively steady process.

Fig. 8 shows the spatial patterns of future precipitation under the RCP4.5 and RCP8.5 scenarios. Under the RCP4.5 scenario, the regionally averaged rate of increase is 2.6 mm decade^{-1}. Large rates occur in the eastern margin and northern margin (Fig. 8g). Areas with precipitation <100 mm exhibit a decrease, and the central part of the Mongolian Plateau exhibits an increase in precipitation, especially for 2085 (Fig. 8a,c,e). Compared to RCP4.5, the increase in precipitation is significant under RCP8.5 at a mean rate of 5.1 mm decade^{-1}, and the increasing precipitation rates along the eastern margin are >12 mm decade^{-1} (Fig. 8h). The spatial differences are apparent among 3 normals, and are especially significant between 2025 and 2085 (Fig. 8b,d,f). Although similar spatial patterns of future precipitation can be seen in the results from the RCP4.5 and RCP8.5 scenarios, they are much stronger for RCP8.5 than for RCP4.5, which suggests that future precipitation will strongly increase under a high emissions scenario (Fig. 8).

To examine the spatial characteristics of future temperature, Fig. 9 depicts the spatial patterns of 3

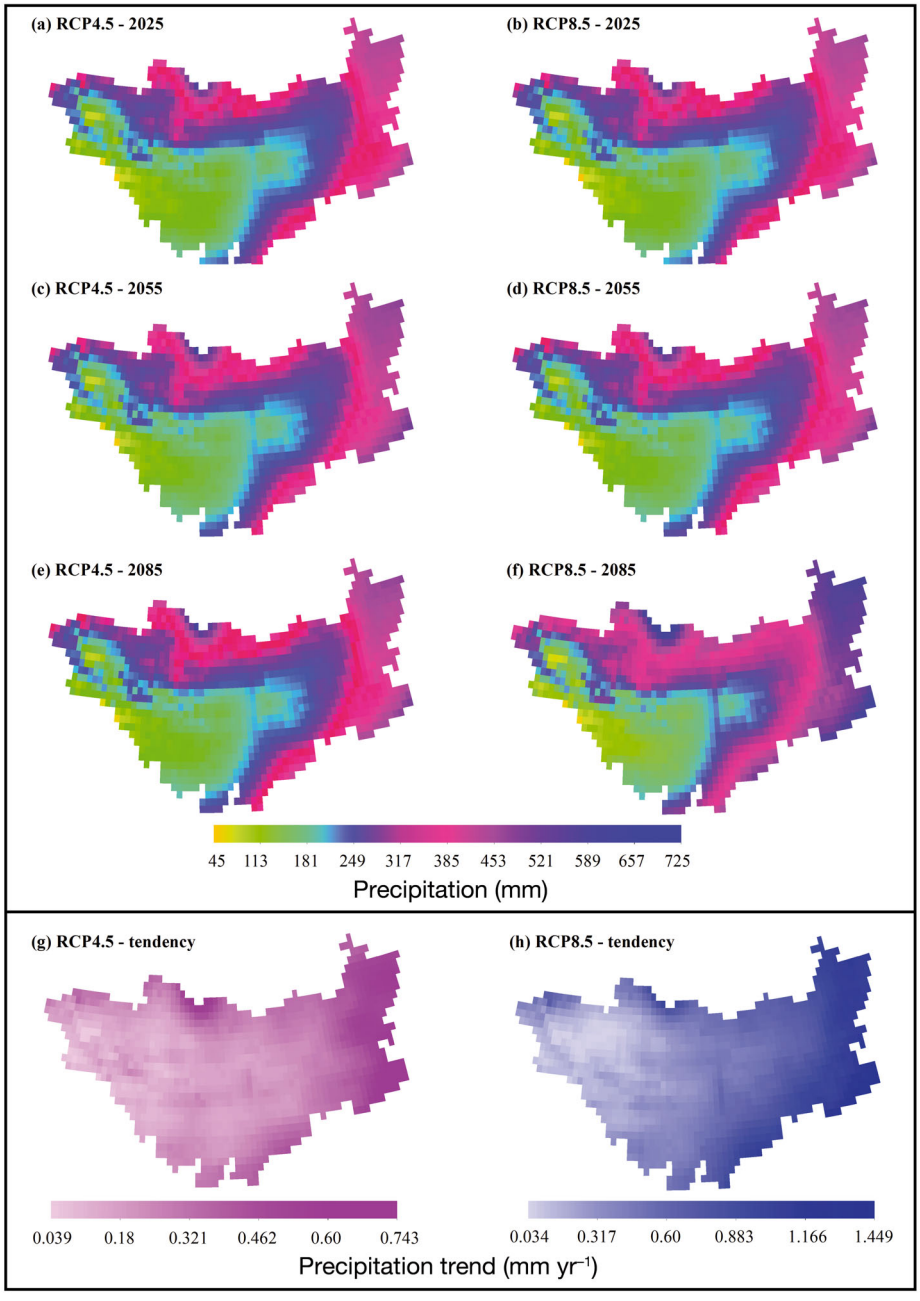

Fig. 8. Spatial patterns for precipitation. (a–f) Projected average annual amount of precipitation for the 2025 (2011–2040), 2055 (2041–2070) and 2085 (2071–2100) periods; (g,h) changing trends based on the multi-model ensemble

normals and long-term trends under RCP4.5 and RCP8.5 emissions scenarios. The warming is ubiquitous, although the spatial distribution of warming rates is complex (Fig. 9g,h). Under RCP4.5, temperature rises greatly over the northern part of the Mongolian Plateau, and there are discernible differences among the 3 normals (Fig. 9a,c,e). That is to say, the cold regions are more sensitive to climate change and have larger warming rates (Fig. 9g). However, the southwestern regions, i.e. the deserts, are still the warmest and show the highest rates of warming. Warming patterns in RCP8.5 are similar to those in RCP4.5, but the changes are more evident and magnitudes are greater. Specifically, the warming rates are in the range of 0.25 to 0.28 versus 0.59 to 0.69°C decade^{-1} under RCP4.5 and RCP8.5, respectively.

Overall, increases in precipitation and temperature can be seen under RCP4.5 and RCP8.5, with larger amplitude changes under RCP8.5. In this context, the Mongolian Plateau will experience significant climate warming and accompanying increased precipitation.

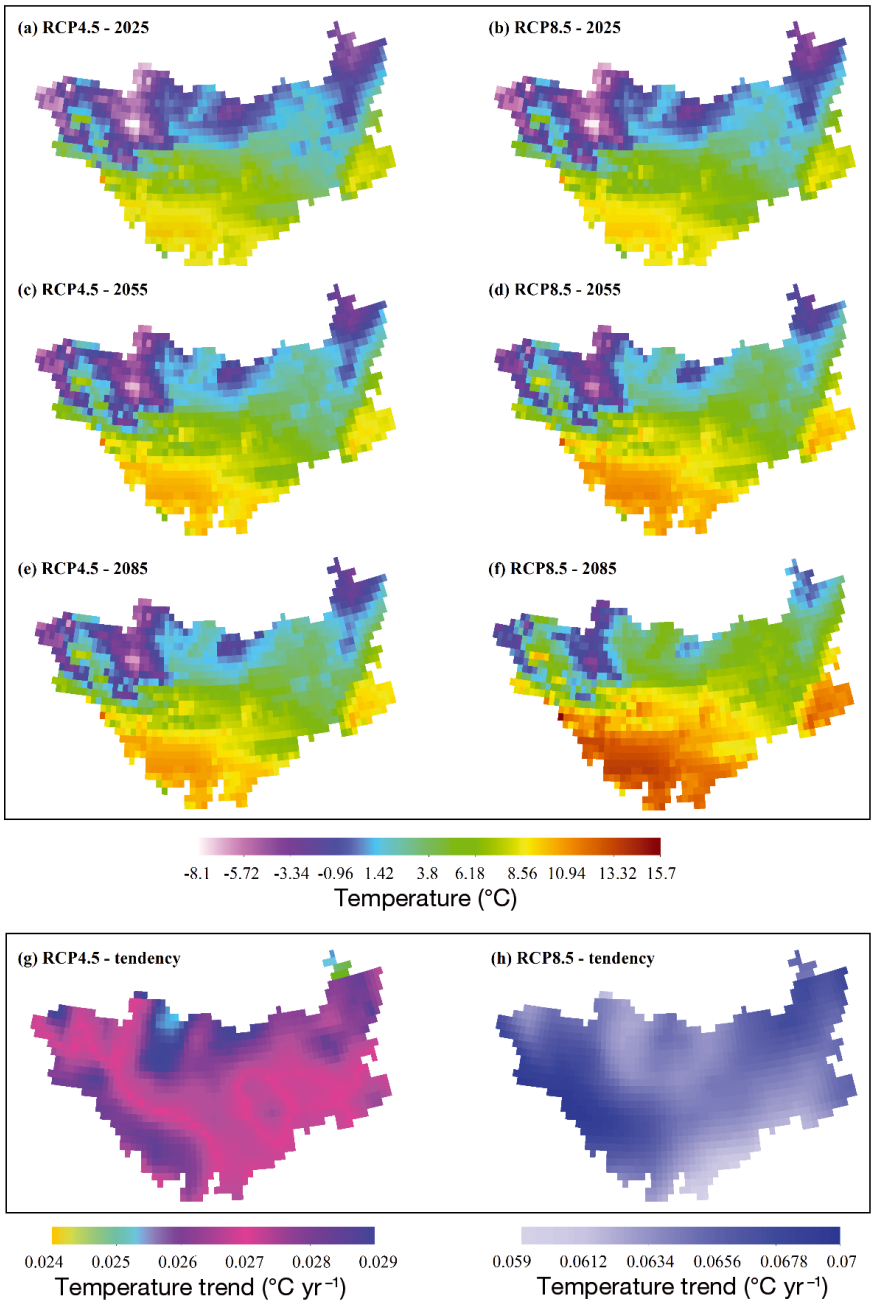

Fig. 9. Spatial patterns for temperature. (a–f) Projected average temperature for the 2025 (2011–2040), 2055 (2041–2070) and 2085 (2071–2100) periods; (g,h) changing trends based on the multi-model ensemble

3.4. Comparison of climate normals over 1961–1990 and 2061–2090

The climatic changes in average annual temperature and amount of precipitation over the periods 1961–1990 (reference period) and 2061–2090 (future prediction) are presented (Figs. 10 & 11). The box chart in Fig. 10 shows seasonal changes in temperature and precipitation. All seasons exhibit an increase in temperature, which is more pronounced in the RCP8.5 than in the RCP4.5 scenario. In addition, the differences between 25 and 75% (i.e. interquartile range) in all seasons except summer decreased for both scenarios, which means that the range in temperature distribution has narrowed. The temperatures in spring and autumn are almost the same for both base values and increments. Winter shows the largest increase over the 2 periods for both scenarios (3.3 and 5.4°C). Seasonal precipitation also shows positive trends, although the frequency distribution of precipitation is narrower. The increases in average precipitation are largest in summer for both scenarios (23 and 28 mm), but the relative increases are lowest (12.8 and 15.9%). However, summer pre-

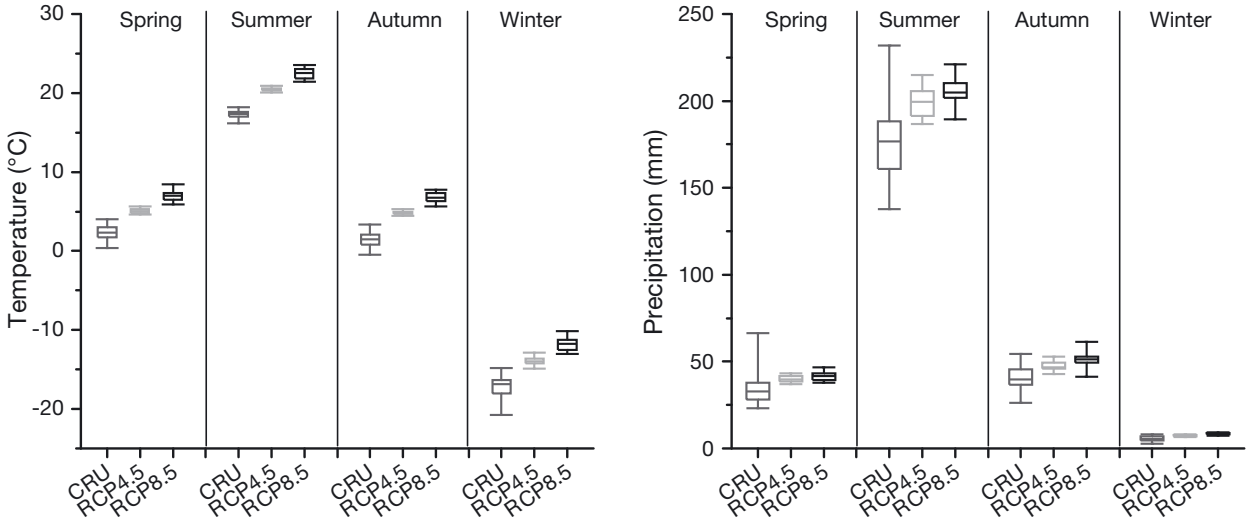

Fig. 10. Seasonal temperatures (left) and amounts of precipitation (right) for the reference period 1961–1990 (Climatic Research Unit [CRU]) and the future period 2061–2090 (representative concentration pathway [RCP] 4.5 and RCP8.5). Central line: mean value; box: 25th and 75th percentile; whiskers: maximum and minimum

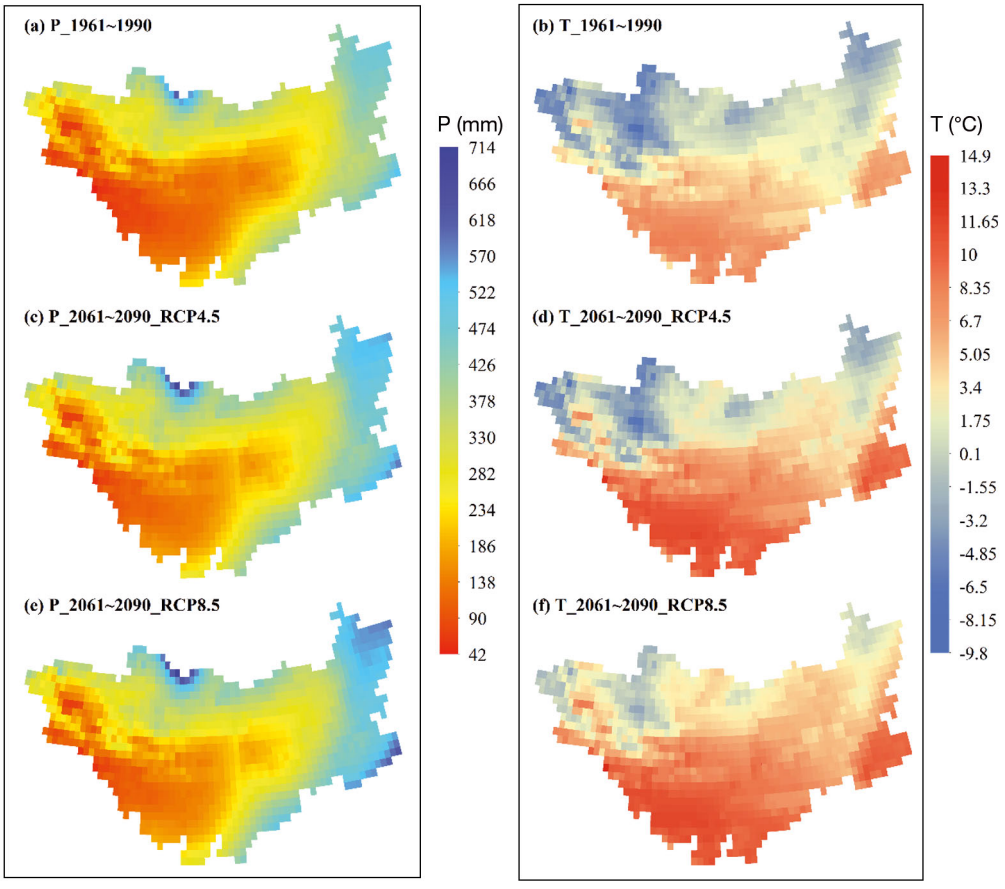

Fig. 11. Spatial distribution of average annual temperature (T, °C) and amount of precipitation (P, mm) for (a,b) the reference period 1961–1990 and (c–f) the future period 2061–2090

cipitation is still dominant in both scenarios, making up about two-thirds of the annual precipitation amount.

Fig. 11 shows that the spatial patterns in precipitation over the reference and future periods are similar. However, the heterogeneity in precipitation across the Mongolian Plateau is evident for both periods. The spatial precipitation patterns show the largest increase in the east (the Greater Higgnan Mountains region) and north (the Eastern Sayan Mountains

region), as evidenced by more blue pixels in Fig. 11c,e. Meanwhile, the southwest shows an increase (fewer red pixels), although the amount of precipitation is still low. The 2 periods show significant spatial differences in temperature, especially in the RCP8.5 scenario. The entire Mongolian Plateau shows an increase in temperature, especially in the north, with only a few blue pixels in the Eastern Sayan Mountains area (Fig. 11d,f). Overall, the warming trend is striking.

4. DISCUSSION

The historical analysis reveals an obvious warming trend throughout the Mongolian Plateau at an average rate of 0.18°C decade^{-1}, which is slightly higher than the mean rate in Central Asia and other semiarid regions (Huang et al. 2012). The warming trend in winter is 0.33°C decade^{-1}, showing an enhanced warming trend. This trend is in agreement with the results of Huang et al. (2012). In addition, the variations in maximum and minimum temperatures were asymmetric during the process of temperature rising. From an ecosystem perspective, the asymmetry in extreme temperatures and the induced narrow range of temperature can have immense environmental consequences and may even lead to cascade effects, particularly in ecologically vulnerable regions.

No significant trend in precipitation was observed, although variations in spring and summer were evident. A large part of the variation in annual precipitation was explained by changes in summer precipitation, as it accounted for a large proportion (67.8%) of the total precipitation. Aridity substantially impacts the pattern and process of water and thermal conditions and leads to environmental changes, such as lake shrinkage and land degradation (Shi et al. 2013, Tao et al. 2015). Tao et al. (2015) indicated that in Mongolia, annual precipitation accounted for 70.4% of lake changes. Water issues are very important to pastoralism on the Mongolian Plateau. Many findings showed that the pastoral nomads have changed their strategy of livestock husbandry to adapt to climate change, and that herders specified changes in the spatial distribution of precipitation and its timing, frequency and intensity as well as water availability as the primary pastoral challenges (Sternberg 2008, Marin 2010, Lkhagvadorj et al. 2013).

Our analysis of future RCP scenarios projects that by 2100, mean annual temperature over the Mongolian Plateau will increase by 3.5 and 7.1°C under the RCP4.5 and RCP8.5 scenarios, respectively. Compared to the climate normal of 3 decades in the last half-century (1961–1990), the future temperature normal of the half-century 2061–2090 will increase by 3.4 and 5.2°C for RCP4.5 and RCP8.5, respectively. This sharp increase merits urgent and intense attention because it is likely to have an important influence on pastures and crops, among other things, as well as on the natural ecosystem on the Mongolian Plateau. Specifically, warmer conditions will affect plant phenology, such as by altering the timing of flowering, the length of the growing season and other developmental events (Cleland et al. 2006).

The analysis of future precipitation shows a weak upward trend, but the magnitude of increase is very small compared to the warming temperature trend. This may cause dry areas to become drier because increased temperature generally would lead to increased evapotranspiration (Huang et al. 2012). However, the combined effects of changed temperature and precipitation are less clear; for example, the East Asian Monsoon could be enhanced by warming surface air temperature over the Mongolian Plateau and could provide increased moisture to the area. Thus, the mechanism of precipitation variation requires further research.

Climate variability and change have increased the vulnerability of herders on the Mongolian Plateau and put pressure on their adaptation strategies (Wang et al. 2013). Unbalanced temperature and precipitation variation will result in pronounced spatial heterogeneity of climate condition (Dong et al. 2013a). Given that the Mongolian Plateau is traditionally an area of farming and agricultural activity, improving the capability to respond and adapt to a warmer environment in the future is an urgent need.

5. CONCLUSIONS

Using the CRU TS3.21 monthly temperature and precipitation dataset, the variation and long-term trends in climate over the past hundred years were evaluated. Future predictions of temperature and precipitation were also analyzed using a multi-model ensemble to understand how the climate will change during the 21st century. The main conclusions of this study are summarized below.

During the past century, the climate of the Mongolian Plateau has shown both warming and drying trends. The average annual amount of precipitation was 254 mm, with a slight decreasing trend (–0.1 mm decade^{-1}). High precipitation mainly occurred in June to August, accounting for 67.8% of annual total

precipitation. Spatially, high precipitation totals appeared in the northern and eastern areas, while low precipitation occurred in the central and southern areas, where the land cover is mainly desert. It should be noted that areas with higher precipitation experienced increasing trends, while those with lower precipitation experienced decreasing trends. Thus, the wet areas got wetter and the dry areas got drier. Long time-series temperature data exhibited strong period fluctuations and a clear upward trend at a rate of 0.18°C decade^{-1}. The increases in minimum temperature, mean temperature and maximum temperature are 1.90, 1.78 and 1.59°C, respectively. Additionally, the winter minimum temperature shows the largest warming trend of all seasons, with a rate of 0.36°C decade^{-1}, showing an asymmetric pattern. A significant south-to-north spatial gradient can be clearly seen. The mountainous areas in the north are characterized by lower temperatures but a higher warming trend.

For predictions of precipitation, by 2100 the increases are 13.3 and 16.1% under the RCP4.5 and RCP8.5 scenarios, respectively, which means that future precipitation will strongly increase under a high emissions scenario. There is an uneven distribution of precipitation, with high precipitation and large increasing rates in the eastern and northern margins of the Mongolian Plateau. Temperature will increase by 3.5 and 7.1°C at the rates of 0.26 and 0.64°C decade^{-1}, respectively, under the 2 scenarios. The warming is ubiquitous, although cold regions are more sensitive to climate change and show higher warming rates than warm regions. It should be noted that the deserts in the southwest are the warmest and have the highest rates of warming.

Compared to the climate normal in 1961–1990, temperature in 2061–2090 exhibits an increase in all seasons, which is more pronounced for RCP8.5 than for RCP4.5. In particular, winter shows the largest increase under both scenarios (3.3 and 5.4°C for RCP4.5 and RCP8.5, respectively). Precipitation also shows positive trends, although the relative increases are not very large (14.2 and 19.2%). The spatial patterns show similar spatial behavior for temperature and precipitation in both scenarios. However, spatial heterogeneity across distinct regions of the Mongolian Plateau is evident.

Given the wetting and significant warming on the Mongolian Plateau, climate change poses a great threat to the area's inhabitants, especially those that practice pastoral husbandry. Adaptation strategies are needed, and adaptation initiatives should be undertaken as soon as possible.

Acknowledgements. This work was supported by the International S&T Cooperation Programme of China (No. 2013DFA91700) through the study 'Climate hazards and risk management in the arid and semi-arid areas of the Mongolian Plateau'. We thank the Climatic Research Unit, University of East Anglia, for providing the CRU TS3.21 dataset. We also acknowledge the British Atmospheric Data Centre for making CMIP5 model outputs available. In addition, the thoughtful comments of Eduardo Zorita and the anonymous reviewers are gratefully acknowledged.

LITERATURE CITED

Ahlstrom A, Schurgers G, Arneth A, Smith B (2012) Robustness and uncertainty in terrestrial ecosystem carbon response to CMIP5 climate change projections. Environ Res Lett 7:044008, doi: 10.1088/1748–9326/7/4/044008

Bastola S, Francois D (2012) Temporal extension of meteorological records for hydrological modelling of Lake Chad basin (Africa) using satellite rainfall data and reanalysis datasets. Meteorol Appl 19:54–70

Berg P, Feldmann H, Panitz HJ (2012) Bias correction of high resolution regional climate model data. J Hydrol (Amst) 448–449:80–92

Bolortsetseg B, Tuvaansuren G (1996) The potential impacts of climate change on pasture and cattle production in Mongolia. Water Air Soil Pollut 92:95–105

Chou SC, Marengo JA, Lyra AA, Sueiro G and others (2012) Downscaling of South America present climate driven by 4-member HadCM3 runs. Clim Dyn 38:635–653

Cleland EE, Chiariello NR, Loarie SR, Mooney HA, Field CB (2006) Diverse responses of phenology to global changes in a grassland ecosystem. PNAS 103:13740–13744

Davi N, Jacoby G, Fang K, Li J, D'Arrigo R, Baatarbileg N, Robinson D (2010) Reconstructing drought variability for Mongolia based on a large-scale tree ring network: 1520–1993. J Geophys Res 115:D22103, doi:10.1029/2010JD013907

Dong JW, Liu JY, Zhang GL, Basara JB, Greene S, Xiao XM (2013a) Climate change affecting temperature and aridity zones: a case study in eastern Inner Mongolia, China from 1960–2008. Theor Appl Climatol 113:561–572

Dong M, Wu T, Wang Z, Xin X, Zhang F (2013b) Simulation of the precipitation and its variation during the 20th century using the BCC climate model (BCC_CSM1.0). J Appl Meteor Sci 24:1–11 (in Chinese)

Ferguson CR, Villarini G (2012) Detecting inhomogeneities in the Twentieth Century Reanalysis over the central United States. J Geophys Res 117:D05123, doi:10.1029/2011JD016988

Gomez-Navarro JJ, Montavez JP, Wagner S, Zorita E (2013) Regional climate palaeosimulation for Europe in the period 1500–1990. 1. model validation. Clim Past 9: 1667–1682

Hao Z, AghaKouchak A, Phillips TJ (2013) Changes in concurrent monthly precipitation and temperature extremes. Environ Res Lett 8:034014

Harris I, Jones PD, Osborn TJ, Lister DH (2014) Updated high-resolution grids of monthly climatic observations – the CRU TS3.10 dataset. Int J Climatol 34:623–642

Haslinger K, Anders I, Hofstaetter M (2013) Regional climate modelling over complex terrain: an evaluation study of COSMO-CLM hindcast model runs for the Greater Alpine Region. Clim Dyn 40:511–529

Huang J, Guan X, Ji F (2012) Enhanced cold-season warming in semi-arid regions. Atmos Chem Phys 12: 5391–5398

Immerzeel W (2008) Historical trends and future predictions of climate variability in the Brahmaputra basin. Int J Climatol 28:243–254

Kynicky J, Brtnicky M, Vavricek D, Bartosova R, Majigsuren U (2009) Permafrost and climatic change in Mongolia. In: Pribullova A, Bicarova S (eds) Sustainable development and bioclimate. Reviewed Conf Proc, Stará Lesná, 5–8 October 2009. Geophysical Institute of the Slovak Academy of Sciences and Slovak Bioclimatological Society of the Slovak Academy of Sciences, p 34–35

Landman WA, Beraki A (2012) Multi-model forecast skill for mid-summer rainfall over southern Africa. Int J Climatol 32:303–314

Lkhagvadorj D, Hauck M, Dulamsuren C, Tsogtbaatar J (2013) Pastoral nomadism in the forest-steppe of the Mongolian Altai under a changing economy and a warming climate. J Arid Environ 88:82–89

Marin A (2010) Riders under storms: contributions of nomadic herders' observations to analysing climate change in Mongolia. Glob Environ Change 20:162–176

Meinshausen M, Smith SJ, Calvin K, Daniel JS and others (2011) The RCP greenhouse gas concentrations and their extensions from 1765 to 2300. Clim Change 109:213–241

Moss RH, Edmonds JA, Hibbard KA, Manning MR and others (2010) The next generation of scenarios for climate change research and assessment. Nature 463:747–756

Ni J (2003) Plant functional types and climate along a precipitation gradient in temperate grasslands, north-east China and south-east Mongolia. J Arid Environ 53: 501–516

Pavlik D, Soehl D, Pluntke T, Mykhnovych A, Bernhofer C (2012) Dynamic downscaling of global climate projections for eastern Europe with a horizontal resolution of 7 km. Environ Earth Sci 65:1475–1482

Philandras CM, Nastos PT, Kapsomenakis J, Douvis KC, Tselioudis G, Zerefos CS (2011) Long term precipitation trends and variability within the Mediterranean region. Nat Hazards Earth Syst Sci 11:3235–3250

Phillips TJ, Gleckler PJ (2006) Evaluation of continental precipitation in 20th century climate simulations: the utility of multimodel statistics. Water Resour Res 42: W03202, doi: 10.1029/2005WR004313

Sato T, Kimura F, Kitoh A (2007) Projection of global warming onto regional precipitation over Mongolia using a regional climate model. J Hydrol (Amst) 333:144–154

Sen Roy S, Sen Roy N (2011) Influence of Pacific decadal oscillation and El Nino Southern oscillation on the summer monsoon precipitation in Myanmar. Int J Climatol 31:14–21

Shi H, Zhou X, Meng F, Bai H (2013) Mongolia and Inner Mongolia LUCC regional differentiation over the past 30 years. J Geo-inf Sci 15:719–725

Sternberg T (2008) Environmental challenges in Mongolia's dryland pastoral landscape. J Arid Environ 72:1294–1304

Tao S, Fang J, Zhao X, Zhao S and others (2015) Rapid loss of lakes on the Mongolian Plateau. Proc Natl Acad Sci USA 112:2281–2286

Taylor KE (2001) Summarizing multiple aspects of model performance in a single diagram. J Geophys Res D 106: 7183–7192

Taylor KE, Stouffer RJ, Meehl GA (2012) An overview of CMIP5 and the experiment design. Bull Am Meteorol Soc 93:485–498

Terink W, Hurkmans RTWL, Torfs PJJF, Uijlenhoet R (2010) Evaluation of a bias correction method applied to downscaled precipitation and temperature reanalysis data for the Rhine basin. Hydrol Earth Syst Sci 14:687–703

Tian F, Herzschuh U, Telford RJ, Mischke S, Van der Meeren T, Krengel M (2014) A modern pollen-climate calibration set from central-western Mongolia and its application to a late glacial-Holocene record. J Biogeogr 41:1909–1922

Wang A, Zeng X (2013) Development of global hourly 0.58° land surface air temperature datasets. J Clim 26: 7676–7691

Wang J, Brown DG, Agrawal A (2013) Climate adaptation, local institutions, and rural livelihoods: a comparative study of herder communities in Mongolia and Inner Mongolia, China. Glob Environ Change 23:1673–1683

Wuebbles D, Meehl G, Hayhoe K, Karl TR and others (2014) CMIP5 climate model analyses: climate extremes in the United States. Bull Am Meteorol Soc 95:571–583

Yue S, Pilon P, Phinney B, Cavadias G (2002) The influence of autocorrelation on the ability to detect trend in hydrological series. Hydrol Processes 16:1807–1829

Editorial responsibility: Eduardo Zorita, Geesthacht, Germany

Submitted: May 8, 2015; Accepted: September 25, 2015
Proofs received from author(s):December 10, 2015